

Improved de-interleaving algorithm of radar pulses based on dual fuzzy vigilance ART

JIANG Wen, FU Xiongjun*, and CHANG Jiayun

School of Information and Electronics, Beijing Institute of Technology, Beijing 100081, China

Abstract: As a core part of the electronic warfare (EW) system, de-interleaving is used to separate interleaved radar signals. The de-interleaving algorithm based on the fuzzy adaptive resonance theory (fuzzy ART) is plagued by the problems of premature saturation and performance improving dilemma. This study proposes a dual fuzzy vigilance ART (DFV-ART) algorithm to address these problems and make the following improvements. Firstly, a correction method is introduced to prevent the network from prematurely saturating; then, the fuzzy vigilance models (FVM) are constructed to replace the conventional vigilance parameter, reducing the error probability in the overlapping region; finally, a dual vigilance mechanism is introduced to solve the performance improving dilemma. Simulation results show that the proposed algorithm could improve the clustering accuracy (quantization error dropped 60%) and the de-interleaving performance (clustering quality increased by 10%) while suppressing the excessive proliferation of categories.

Keywords: fuzzy adaptive resonance theory (fuzzy ART), de-interleaving, dual vigilance mechanism.

DOI: 10.23919/JSEE.2020.000008

1. Introduction

The main purpose of the electronic warfare (EW) system is to intercept emission signals, de-interleave the intercepted signals and identify surrounding threatening emitters. With the development of EW environment, intercepted signals are interleaved into complex pulse trains. In order to separate the pulse train effectively, the advanced de-interleaving theory becomes very critical.

De-interleaving approaches in literature can be divided into two categories: pulse repetition interval (PRI) analysis and feature clustering. Methods based on the PRI analysis include the PRI training method [1], cumulative differences of PRI histograms (CDIF) [2], sequential differences of PRI histograms (SDIF) [3], and hidden Markov

models [4–7]. As for clustering-based approaches, the improved algorithm was proposed by Liu and Zhang [8] using clustering and SDIF, and by Guo [9] and Bradley [10] using K-means. Notably, a two-stage clustering technique proposed by Gencol [11] also achieves good results.

Compared with the conventional clustering methods, the fuzzy adaptive resonance theory (fuzzy ART) [12,13] has great advantages in automatic processing and intelligent learning. These advantages make the algorithm suit for automatic de-interleaving of radar pulses [14]. However, the applications of the fuzzy ART to de-interleaving process are still limited. In [14], authors demonstrated that the fuzzy ART suits for radar pulse de-interleaving. On this basis, Ata'a and Abdullah [15] realized the clustering of radar features, including pulse width (PW), pulse frequency (PF) and angle-of-arrival (AOA), using the fuzzy ART network. In [16], Gencol et al. proposed a pulse amplitude (PA) tracking algorithm and used the estimated PA as a fourth information source incorporating with other parameters to assist the clustering of radar features.

The studies mentioned above all focus on how to use the fuzzy ART to de-interleave radar signals, ignoring the improvement of the algorithm itself. Since the mechanisms of the ART network are triggered by a vigilance test under the control of a stable vigilance parameter, it is very difficult for ART systems to address the problems of premature saturation [17] and performance improving dilemma [18] during the de-interleaving process. This paper augments the fuzzy ART de-interleaving systems by making the following improvements: first, a correction method is introduced to prevent the network from prematurely saturating and improve clustering accuracy; then, fuzzy vigilance models (FVM) are constructed to replace the conventional vigilance parameter, reducing the error probability in overlapping region; finally, a dual vigilance mechanism is introduced to address the performance improving dilemma. Simulation results show that the proposed algorithm could improve the clustering accuracy and address the dilemma in the fuzzy ART de-interleaving systems.

Manuscript received July 03, 2019.

*Corresponding author.

This work was supported by the National Natural Science Foundation of China (61571043) and the 111 Project of China (B14010).

2. Related work

The fuzzy ART is widely used for a variety of issues, such as clustering [19,20], vector quantization [21–23] and classification [24–27]. In this section, we briefly introduce the algorithm of the fuzzy ART and the mathematical model of Type-2 fuzzy sets (T2-FSs), paving the way for the subsequent research.

2.1 Fuzzy ART

The fuzzy ART consists of the following three layers: F_0 , F_1 , and F_2 , as shown in Fig. 1. F_0 is used to normalize and complement-code the inputs. F_1 is used for calculating the membership between the input and the neurons in layer F_2 . The fuzzy ART selects the winning neuron by comparing neurons' memberships and updates the weight of the winner. Finally, the outputs of layer F_2 are the active categories.

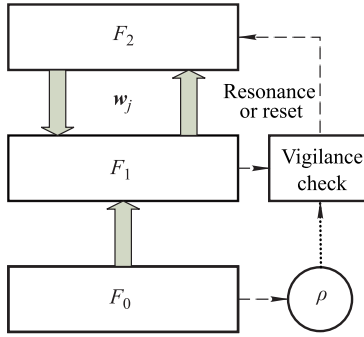


Fig. 1 Fuzzy ART architecture

The algorithm proceeds as follows:

(i) Present normalized and complement-coded input \mathbf{I} to F_1 and calculate the choice function T_j for category j in F_2 :

$$T_j = \frac{\|\mathbf{I} \wedge \mathbf{w}_j\|_1}{\alpha + \|\mathbf{w}_j\|_1}, \quad j = 1, \dots, N \quad (1)$$

where $\mathbf{I} = (\mathbf{a}, \mathbf{a}^c)$, \mathbf{a} is the original input before F_0 -layer processing; \mathbf{w}_j is the adaptive weight vector of category j ; α is the choice parameter; and N is the number of the categories in layer F_2 .

(ii) Select the winner J by using a winner-take-all competition:

$$T_J = \max\{T_j\}, \quad j = 1, \dots, N. \quad (2)$$

(iii) Perform a vigilance check by using the match criterion:

$$\frac{\|\mathbf{I} \wedge \mathbf{w}_J\|_1}{\|\mathbf{I}\|_1} \geq \rho. \quad (3)$$

(iv) If J satisfies the match criterion, then update its weights:

$$\mathbf{w}_J^{\text{new}} = \beta(\mathbf{I} \wedge \mathbf{w}_J^{\text{old}}) + (1 - \beta)\mathbf{w}_J^{\text{old}}. \quad (4)$$

(v) If J fails, then reset it and repeat (ii) until a winner passes. If no existing category succeeds, then a new category should be created.

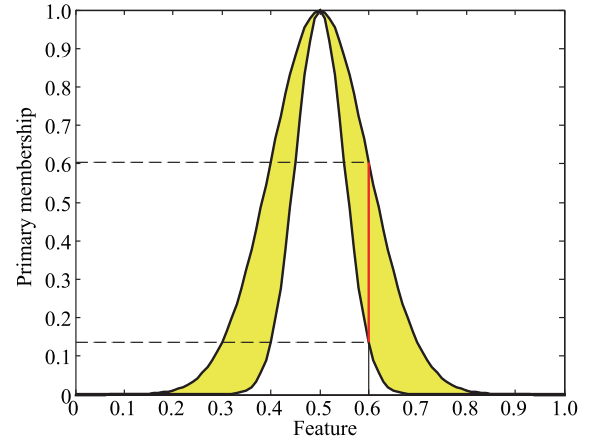
2.2 T2-FSs

The T2-FSs [28–30] in a universe of discourse \mathbf{X} , denoted as $\tilde{\mathbf{A}}$, are characterized by Type-2 membership function $\mu_{\tilde{\mathbf{A}}}(x, \mu)$, where $x \in \mathbf{X}$ and $\mu \in J_{\mathbf{X}} \subseteq [0, 1]$:

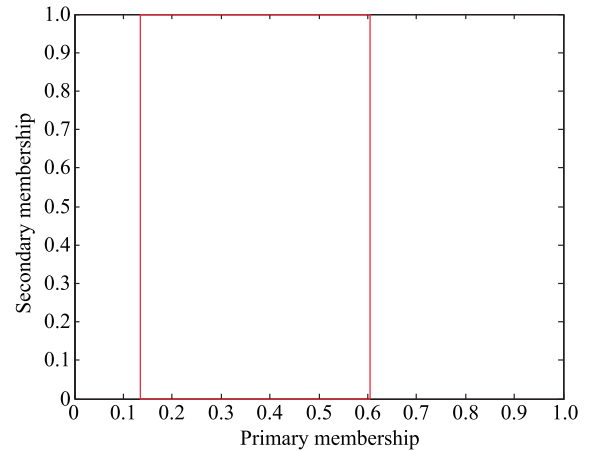
$$\tilde{\mathbf{A}} = \int_{x \in \mathbf{X}} \int_{\mu \in J_{\mathbf{X}}} \mu_{\tilde{\mathbf{A}}}(x, \mu) / (x, \mu) \quad (5)$$

where \int denotes the union over all admissible x and μ , $0 \leq \mu_{\tilde{\mathbf{A}}}(x, \mu) \leq 1$ and $J_{\mathbf{X}}$ is the primary membership of x which is the domain of the secondary membership [28].

Fig. 2(a) illustrates a Gaussian T2-FSs with the fixed mean and uncertain standard deviation [29]. The distribution of the primary membership, called the footprint of uncertainty (FOU), is shown in the yellow area and the FOU is bounded by lower membership function (LMF) and upper membership function (UMF). The secondary membership, shown in Fig. 2(b), can be obtained by taking a vertical slice of $\mu_{\tilde{\mathbf{A}}}(x, \mu)$, red line in Fig. 2(a).



(a) Gaussian primary membership



(b) Interval secondary membership

Fig. 2 Gaussian T2-FS

For these T2-FSSs, the centroid [30] of the FOU could be fully characterized by its left and right endpoints [30]. It is worth pointing out that the centroid in the fuzzy vigilance model constructed in this paper is precisely the distribution center of vigilance parameters. Therefore, the calculation of the centroid is of great significance.

3. Problem statement

3.1 Premature saturation

The fuzzy ART network has the characteristic of fast convergence. The network will be saturated after a small amount of training, making weight vectors no longer update with the input data. Since weight vectors represent the clusters of the ART network, premature saturation will affect the accuracy of clusters. In order to improve the clustering accuracy, it is very important to prevent the network from prematurely saturating.

3.2 Performance improving dilemma

In the fuzzy ART model, categories in layer F_2 overlap each other, as shown in Fig. 3(a), making higher error probability in the overlapping region, as shown in Fig. 3(b).

Since the mechanisms of the model are controlled by a stable vigilance parameter ρ , it needs to increase the value of ρ to reduce the error probability. However, the increased ρ will cause the proliferation problem, as shown in Fig. 3(c), resulting in a decrease in sorting performance.

Therefore, the conventional vigilance becomes a double-edged sword for improving the sorting performance, and it is very critical for ART de-interleaving systems to choose a new vigilance model with adaptive characteristics to replace the conventional vigilance parameter.

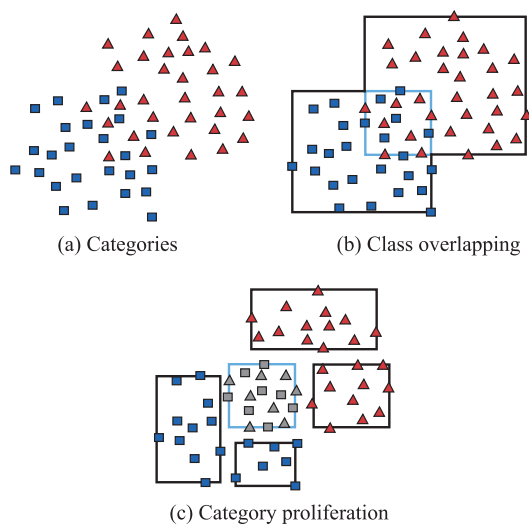


Fig. 3 Performance improving dilemma

4. DFV-ART algorithm

To solve the problems mentioned above, a dual fuzzy vigilance ART (DFV-ART) algorithm is proposed by referencing the T2-FSSs [28–31] and the dual vigilance theory [32]. Compared with the traditional fuzzy ART, the advantages and innovations of the DFV-ART are shown as follows.

(i) The DFV-ART prevents the ART network from prematurely saturating. Through the proposed correction method, the utilization of different features is obviously increased, and the clustering accuracy improves significantly.

(ii) The DFV-ART uses the adaptive vigilance threshold to replace the traditional fixed vigilance parameter, reducing the error probability in the overlapping region. Through the construction of new vigilance models, presented as the FVM, the DFV-ART selects different and appropriate vigilance thresholds for different signal categories.

(iii) The DFV-ART overcomes the performance bottleneck of the fuzzy ART de-interleaving systems. Through the introduction of the dual vigilance mechanism, the DFV-ART suppresses the excessive proliferation and addresses the performance improving dilemma.

4.1 Correction method

In the fuzzy ART sorting systems, the similarity of two radar feature vectors is measured by using fuzzy operations. However, fuzzy operations have the following limitations. (i) When a feature is far greater than the others, this feature, called the super factor (SF), will make other features lose the contribution to category difference in fuzzy operating. (ii) The greater the number of the SF is, the easier it is for the fuzzy ART to saturate prematurely. To break these limitations and improve the clustering accuracy, a correction method is introduced to reduce the differences among the features.

For a more intuitive analysis, we build the following scenario: $\mathbf{a} = (a_1, \dots, a_M)$ is the input radar feature vector and M is its dimension; a_1, a_2, \dots, a_k are the SF, whose values are all $100a$ ($a > 0$); the values of the rest are all a (for example, the value of the PF, in MHz, is often 100 times larger than the PW, in μs). After the normalization of \mathbf{a} , the normalized SF b_i ($i = 1, \dots, k$) can be expressed as follows:

$$b_i = \frac{100a}{\sqrt{k(100a)^2 + (M-k)a^2}} = \frac{100}{\sqrt{M + 999.9k}}. \quad (6)$$

Since the 1-norm of $\mathbf{I} = (\mathbf{a}, \mathbf{a}^c)$ is M after the complement-coding, the proportion of the SF in the accu-

mulation is

$$\delta = \frac{100k}{M\sqrt{M+9999k}} + \dots + \frac{M-k}{M} \left(1 - \frac{1}{\sqrt{M+9999k}} \right). \quad (7)$$

Since M is a fixed value, the value of k determines the size of δ . As $k \rightarrow 0.5M$, $\delta \rightarrow 1$. In this condition, the SF makes it very difficult for other features to affect the result of vigilance check. As $k \rightarrow 0$, $\delta \rightarrow 0.5$. At this time, each feature in \mathbf{I} contributes to distinguish the category differences. Therefore, it is an effective method to prevent the fuzzy ART from prematurely saturating by reducing the differences among the features. To achieve this goal, a correction method is proposed and the method is divided into two steps.

(i) First, correct the dynamic range of each feature.

Assuming that the standard deviation of the i th feature is σ_i , the initially corrected input can be expressed as follows:

$$\mathbf{a} = (b_1, b_2, \dots, b_M),$$

$$b_i = \frac{a_i}{\sigma_i}, \quad i = 1, \dots, M. \quad (8)$$

(ii) Second, correct the magnitude of each feature.

Assuming that the mean of the i th feature is μ_i , the correction criterion μ can be obtained by

$$\mu = \min\{\mu_i\}, \quad i = 1, \dots, M. \quad (9)$$

The correcting factor can be obtained by using the correction criterion μ :

$$\zeta_i = 10^n \cdot \sigma_i, \quad i = 1, \dots, M \quad (10)$$

where n satisfies $10^n \leq \frac{\mu_i}{\mu} < 10^{n+1}$. The final result of the correction can be expressed as follows:

$$\mathbf{a} = (c_1, c_2, \dots, c_M),$$

$$c_i = \frac{b_i}{\zeta_i} = \frac{b_i}{10^n \cdot \sigma_i}, \quad i = 1, \dots, M. \quad (11)$$

4.2 FVM

(i) Construction of the FVM

The parameters of the FVM are set as follows: $\mathbf{I} = (I_1, \dots, I_{2M})$ is corrected, normalized and complement-coded input, $[m_1, m_2]$ is the range of the fuzzifier m [31], J is the winning category and \mathbf{w}_J is the adaptive weight vector of J .

The FVM is a kind of T2-FSSs, obtained by fuzzy processing of the distance between \mathbf{I} and \mathbf{w}_J . This type of

T2-FSSs is used to show the distribution of vigilance parameters, and the distribution, yellow region in Fig. 4, is bounded by the LMF $\underline{\rho}$ and the UMF $\bar{\rho}$, which can be expressed as follows:

$$\underline{\rho} = 1 - e^{-m_1 d}$$

$$\bar{\rho} = 1 - e^{-m_2 d} \quad (12)$$

where $d = |\mathbf{w}_J - \mathbf{I}|$ is a distance vector between \mathbf{I} and \mathbf{w}_J .

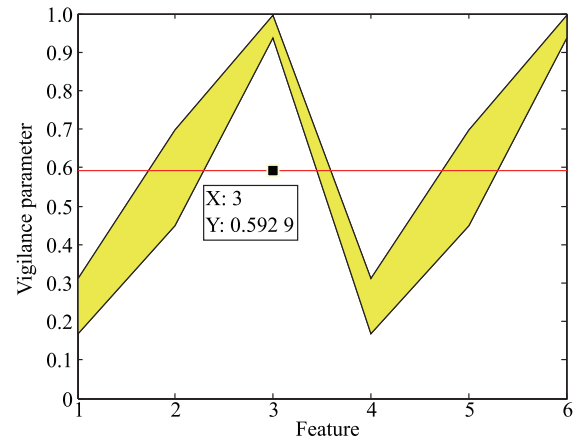
(ii) Calculation of the vigilance threshold

When the input is \mathbf{I} and the winner is J , the distribution center ρ^* can be obtained by calculating the centroid of the FVM:

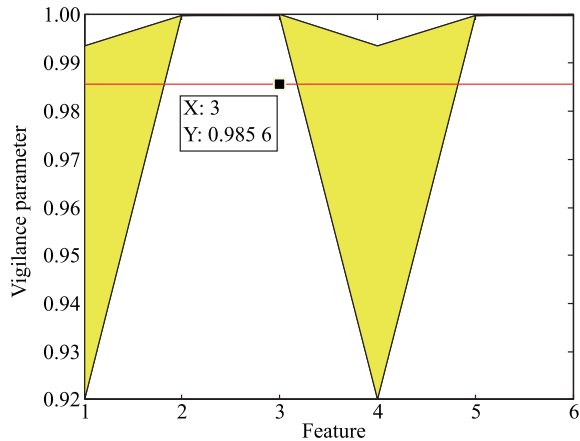
$$\rho^* = \frac{1}{2}(\underline{\rho} + \bar{\rho}). \quad (13)$$

At this point, the vigilance threshold ρ^* , the red line in Fig. 4, is constructed as follows:

$$\rho^* = \frac{1}{2M} \|\rho^*\|_1 = 1 - \frac{1}{4M} \sum_{k=1}^{2M} (e^{-m_1 d_k} + e^{-m_2 d_k}). \quad (14)$$



(a) Same categories



(b) Different categories

Fig. 4 FVM

The two figures in Fig. 4 show the distribution of vigilance parameters. When the categories of the input and the winner are the same, in Fig. 4(a), the vigilance threshold is reduced to 0.593. When the categories are different, in Fig. 4(b), the vigilance threshold is raised to 0.986. The comparison results illustrate that the FVM improves the structure of the fuzzy ART by choosing different and suitable thresholds for different categories.

4.3 Dual vigilance mechanism

To address the performance improving dilemma, vigilance thresholds should be further adjusted according to the category difference between the input and the winner. For this goal, another vigilance, presented as the category vigilance, is introduced to predict the status of the fuzzy ART network and assist the adjustment of vigilance thresholds.

The dual vigilance mechanism is proceeded as follows.

(i) First, initialize the category vigilance ρ_j ($j = 1, \dots, N$).

If the category j is sorted for the first time, ρ_j is initialized to

$$\rho_j = \rho^*. \quad (15)$$

(ii) Second, predict the status of the fuzzy ART system. The prediction uses the following match criterion:

$$\frac{\|\rho_j \wedge \rho^*\|_1}{\|\rho^*\|_1} \geq \rho^* \quad (16)$$

where $\rho^* = (\rho_1^*, \dots, \rho_{2M}^*)$ and $\rho^* = \max_{i=1, \dots, 2M} [\rho_i^*]$.

(iii) Finally, adjust the category vigilance ρ_j and get the optimal vigilance parameter ρ .

If the match criterion is satisfied, the ART system will trigger resonant state after the vigilance check. In this condition, ρ_j should be updated in advance to

$$\rho_j^{\text{new}} = \beta(\rho^* \wedge \rho_j^{\text{old}}) + (1 - \beta)\rho_j^{\text{old}}. \quad (17)$$

The optimal vigilance parameter ρ predicted by this paper is

$$\rho = \frac{1}{2M} \|\rho_j^{\text{new}}\|_1. \quad (18)$$

If the match criterion fails, the ART system will trigger the reset state and the predicted ρ can be obtained by

$$\rho = \max_{i=1, \dots, 2M} [\rho_i^*]. \quad (19)$$

4.4 Flowchart

The flowchart of the DFV-ART is shown in Fig. 5.

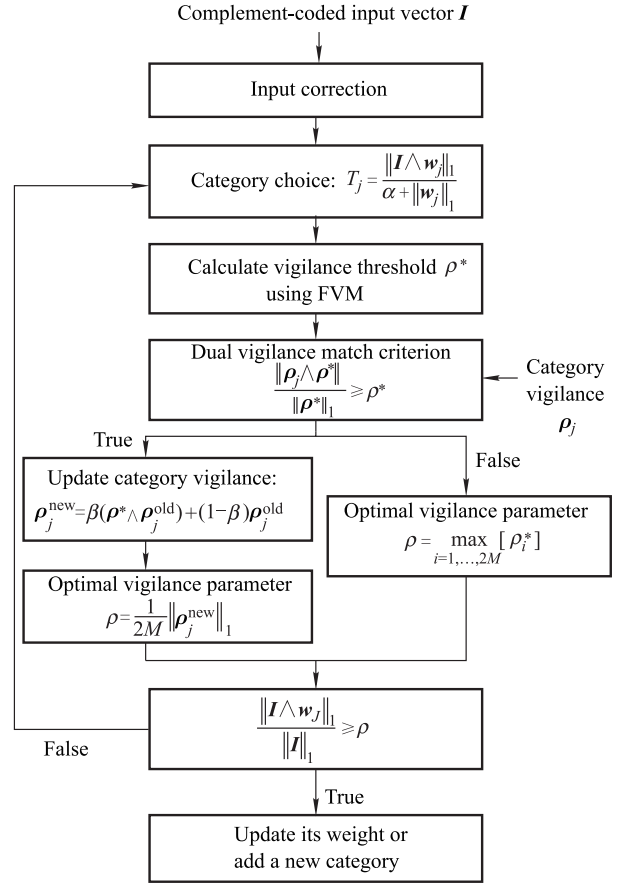


Fig. 5 Flowchart of DFV-ART

5. Simulation and discussion

In the following section, we present the assessment results for the DFV-ART algorithm applied to radar pulse de-interleaving. In this sense, a comparative study with the fuzzy ART [16], Type-1 fuzzy ART (T1-FA) [31] and the DFV-ART is accomplished. The evaluation involves the clustering quality (CQ) [16], quantization error (QE) [16] of clusters, number of training pulses and the quantity of categories created by ART systems. It is worth pointing out that each experiment in the comparative study is repeated 100 times under the condition that the order of the input presentation is random. The result of each experiment is the mean of 100 repetitions.

In these experiments, α and β are set to 0.1 and 0.6 respectively, and a grid search is used for parameter tuning. The $[0, 1]$ interval with a step size of 0.001 is used for searching the vigilance parameter ρ of the fuzzy ART. Finally, the fuzzifier m in T1-FA is set to 2 000 and the range $[m_1, m_2]$ for DT2-FA is set to $[700, 800]$.

5.1 Experimental data

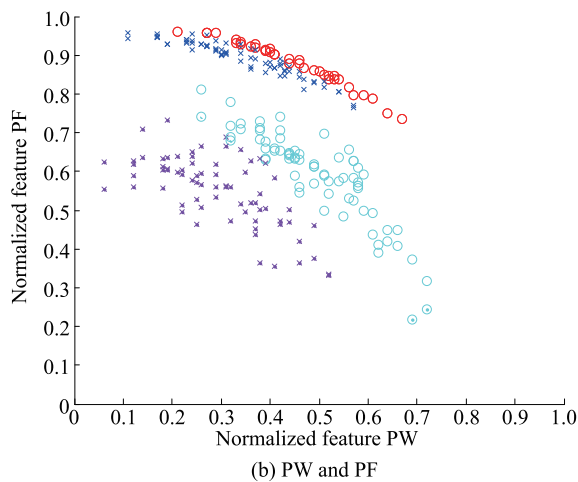
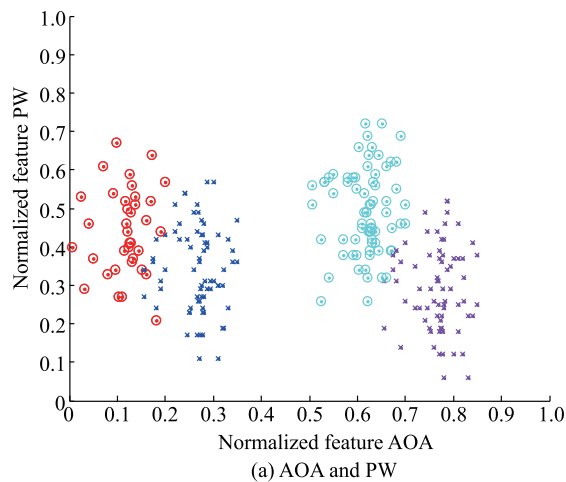
The experimental data include 13 kinds of radar signals, and the parameters of the signals are shown in Table 1.

The parameters contain AOA, PW, PF and their codes of complement.

Table 1 13 radars' parameters

Radar	AOA/(°)	PW/ μ s	PF/MHz	PRI/ μ s
1	55	2	1 000	Constant: 270
2	85	3.5	1 200	Constant: 1 500
3	115	5	1 400	Grops: 416/458/471/594
4	145	6.5	1 600	Jitter: 15%; Center: 750
5	175	8	1 800	Hopping: 10%; Center: 1 100
6	55	3.5	1 300	Constant: 270
7	115	3.5	1 300	Constant: 270
8	145	3.5	1 300	Constant: 270
9	175	3.5	1 300	Constant: 270
10	115	6.5	1 000	Constant: 500
11	115	6.5	1 200	Constant: 500
12	115	6.5	1 400	Constant: 500
13	115	6.5	1 600	Constant: 500

The distribution of normalized radar features is shown in Fig. 6. To make the image more clear, only four of the 13 signals are shown.



○ : Radar 1; × : Radar 2;
○ : Radar 3; × : Radar 4.

Fig. 6 Distribution of radar features

5.2 Result and discussion

Fig. 7 and Fig. 8 show the simulation results of the comparative study. It is worth pointing out that the deinterleaving performance of the fuzzy ART without correcting the input is shown in Fig. 7(a). As for the simulations in other figures, the input feature vectors all are corrected by using the proposed method.

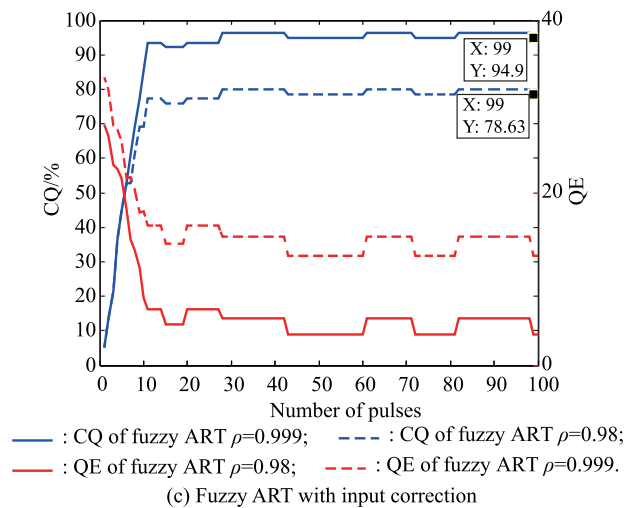
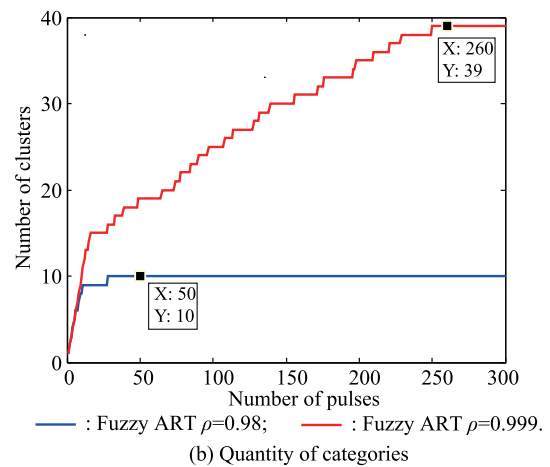
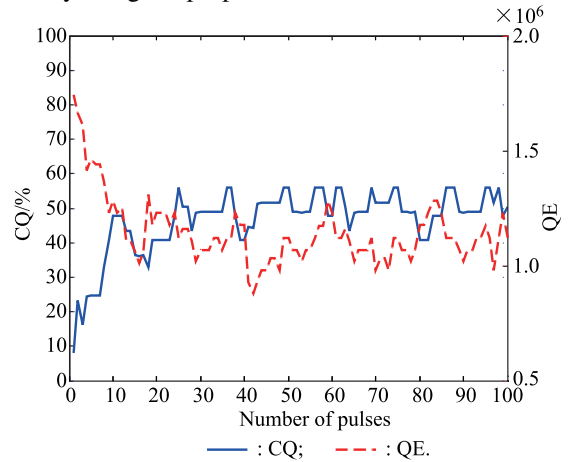


Fig. 7 Performance of fuzzy ART

The results in Fig. 7(a) illustrate that the fuzzy ART without the input correction has poor performance. The QE of clusters fluctuates around 1.2×10^6 and the clustering quality is 50%. Since the dynamic ranges of different features are significantly different before the correction, the fuzzy ART is more sensitive to features with a large dynamic range, ignoring the influence of the others. Therefore, without the correction, the de-interleaving performance of the fuzzy ART is seriously affected.

After using the correction method, from Fig. 7(b) to Fig. 8(c), the fuzzy ART takes advantages of all the features to get the network fully trained before it saturates. Therefore, the QE is rapidly reduced and the CQ is significantly improved. The comparison results illustrate that the proposed method could improve the clustering accuracy effectively. The de-interleaving performance of the fuzzy ART with different ρ is shown in Fig. 7(c), where ρ is set to 0.98 and 0.999 respectively. The results illustrate that ρ becomes a double-edged sword for improving the de-interleaving performance. When the value of ρ increases from 0.98 to 0.999, the CQ is increased from 78.63% to 94.4%, and the QE is reduced from 10.62 to 3.6. However, the increased ρ causes an excessive proliferation of clusters, the red curve in Fig. 7(b), making the number of clusters much higher than the quantity of signal categories.

Therefore, the traditional vigilance parameter becomes an unfavorable factor that limits the performance improving of the fuzzy ART, and it is very critical for ART systems to choose a new vigilance model to replace the conventional vigilance parameter.

The T1-FA and DFV-ART both construct a vigilance model with adaptive characteristics, and the performance of the two algorithms are shown in Fig. 8.

The CQ of T1-FA reaches 82.8% while the QE decreases to 7.158, as shown in Fig. 8(c). Since the vigilance parameter could be adaptively adjusted, the clusters of T1-FA do not proliferate as the training pulses increase, the blue curve in Fig. 8(b), making the quantity of the active categories gradually stabilize to 11. The results illustrate that the T1-FA can suppress the excessive proliferation and has a better sorting effect than the fuzzy ART. However, the performance of the T1-FA is limited by the fuzzifier, as shown in Fig. 8(a), resulting in an upper limit on the improvement of sorting performance.

The DFV-ART proposed by this paper breaks this limitation and obtains the optimal sorting performance. Due to the construction of the fuzzy vigilance model, the DFV-ART selects different and appropriate vigilance thresholds for different signal categories. It not only further improves the clustering performance, but also makes the algorithm more stable.

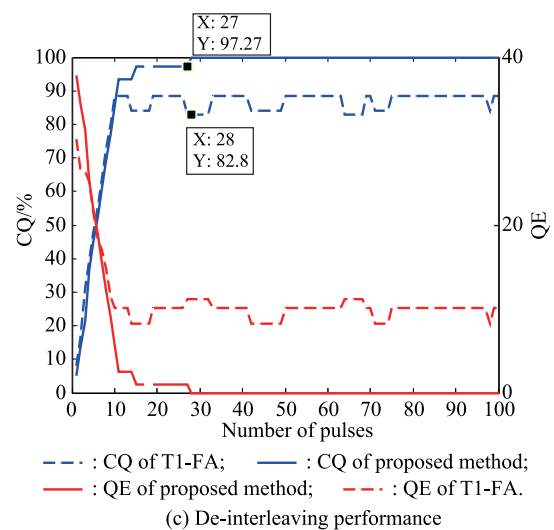
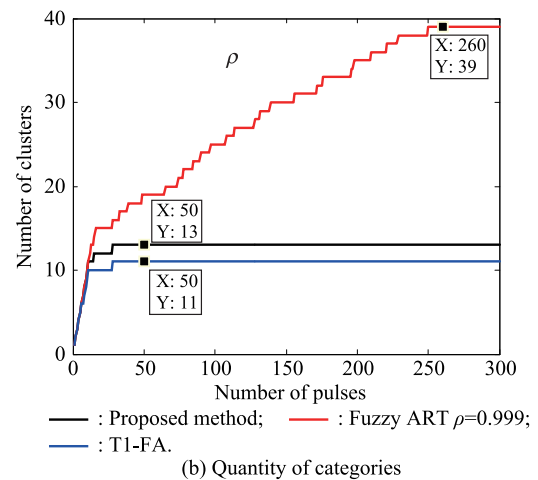
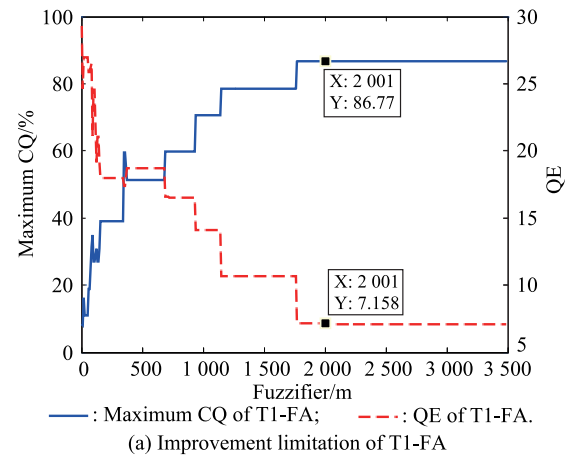


Fig. 8 Performance of T1-FA and DFV-ART

The stability of the DFV-ART makes clusters' number stabilize at 13, as shown by the black line in Fig. 8(b), which is equal to the quantity of signal categories. The performance comparison of the DFV-ART and T1-FA is shown in Fig. 8(c). Due to the mechanism of dual vigi-

lance, the DFV-ART breaks the limitation of the performance improving. The mechanism makes the input data gradually approach the clustering centers, resulting in the gradual aggregation of the similar data. Therefore, comparing with the T1-FA, the CQ of the DFV-ART increases from 82% to 97%, and the performance improves significantly.

Compared with the other algorithms, the proposed algorithm can correctly sort all 13 types of the input signals while suppressing the excessive proliferation. Therefore, the algorithm proposed by this paper achieves the optimal effect.

The de-interleaving performance is analyzed above, and then we will further analyze the computational complexity of the three algorithms. The computational complexity is derived from four parts (the symbols in parentheses represent the amount of calculation for this part): data initialization (C_I), membership calculation ($N \times C_M$), vigilance check (C_V) and weights update (C_U). Therefore, the computational complexity of the three algorithms is shown in Table 2.

Table 2 Computational complexity

Algorithm	Computational complexity
Fuzzy ART	$N_1 \times C_M + C_I + C_V + C_U$
T1-FA	$N_2 \times C_M + C_I + 2C_V + C_U$
DFV-ART	$N_3 \times C_M + 2C_I + 4C_V + C_U$

The membership calculation part needs to calculate the membership between the input and N categories in layer F_2 , as shown in (1). Each time the winning category is searched, the membership calculation part needs to be calculated repeatedly N times, while the other parts are calculated only once. Therefore, the membership calculation part has the largest amount of calculation (more than 50%), and the calculation amount is related to the number N of categories in layer F_2 . Due to the proliferation problem, shown in Fig. 7, the categories' number N_1 of the fuzzy ART is larger than that of T1-FA (N_2) and DFV-ART (N_3). Therefore, the fuzzy ART has the highest complexity. Due to the introduction of correction methods and dual vigilance mechanisms, the calculation amount of the DFV-ART is twice larger than that of the T1-FA in the parts of data initialization and vigilance check. Therefore, the computational complexity of the DFV-ART is slightly higher than that of the T1-FA while the performance is improved significantly.

In view of the above advantages, the DFV-ART has great advantages in clustering and vector quantization, which makes it suitable for de-interleaving similar signals. With the development of modern EW, emission signals become complex and variable, making the signals intercepted by the EW systems interleave into complex pulse trains. To separate the pulse trains effectively, it needs the advanced

de-interleaving algorithm, and the DFV-ART has a huge advantage in this respect. Therefore, the research on the DFV-ART is very promising.

6. Conclusions

This work presents the idea of correcting the input and using new vigilance models to replace the conventional vigilance parameter, which is shown in the DFV-ART, and improves the clustering accuracy and addresses the performance improving dilemma. It is accomplished by correcting the input feature vectors, calculating the vigilance threshold from the FVM and using the dual vigilance mechanism to adjust the threshold. Simulation results show that the proposed algorithm can improve the clustering accuracy and address the dilemma in fuzzy ART de-interleaving systems.

References

- [1] GE Z P, SUN X. Improved algorithm of radar pulse repetition interval de-interleaving based on pulse correlation. *IEEE Access*, 2019, 7: 30126–30134.
- [2] MOSTAFA B, MOHAMMAD H S. A new approach to pulse de-interleaving based on adaptive thresholding. *Turkish Journal of Electrical Engineering and Computer*, 2017, 25(5): 3827–3838.
- [3] MOSTAFA B, MOHAMMAD H S. A new method for detecting jittered PRI in histogram-based methods. *Turkish Journal of Electrical Engineering and Computer*, 2018, 26(3): 1214–1224.
- [4] LOGOTHETIS A, KRISHNAMURTHY V. An interval-amplitude algorithm for de-interleaving stochastic pulse train sources. *IEEE Trans. on Signal Processing*, 1998, 46(5): 1344–1350.
- [5] LIU Y C, ZHANG Q Y. Improved method for de-interleaving radar signals and estimating PRI values. *IET Radar, Sonar and Navigation*, 2018, 12(5): 506–514.
- [6] MAHMOUD K, DELARAM A, MANSOUR P A. A novel method of de-interleaving pulse repetition interval modulated sparse sequences in noisy environment. *IEICE Trans. on Fundamentals of Electronics Communications and Computer Sciences*, 2014, 97(5): 1136–1139.
- [7] TORUN O, MEHMET B K, HAKAN A, et al. De-interleaving of radar signals with stagger PRI and dwell-switch PRI types. *Proc. of the 25th Signal Processing and Communications Applications Conference*, 2017: 89–97.
- [8] LIU Y C, ZHANG Q Y. Improved method for de-interleaving radar signals and estimating PRI values. *IET Radar, Sonar and Navigation*, 2018, 12(5): 506–514.
- [9] GUO N Q, ZHANG N X, LI N Z. SVC & K-means and type-entropy based de-interleaving/recognition system of radar pulses. *Proc. of the IEEE International Conference on Information Acquisition*, 2006: 742–747.
- [10] BRADLEY P, FAYYAD U. Refining initial points for K-means clustering. *Proc. of the 15th International Conference on Machine Learning*, 1998: 91–99.
- [11] GENCOL K. A two-stage de-interleaving technique for clustering of radar pulses. *Proc. of the 25th Signal Processing and Communications Applications Conference*, 2017: 331–341.
- [12] CARPENTER G A, GROSSBERG S, ROSEN D B. Fuzzy ART: fast stable learning and categorization of analog patterns

- by an adaptive resonance system. *Neural Networks*, 1991, 4(6): 759–771.
- [13] SILVA L E B D, WUNSCH D C. Multi-prototype local density-based hierarchical clustering. *Proc. of the International Joint Conference on Neural Networks*, 2015: 1–9.
- [14] GRANGER E, SAVARIA Y, LAVOIE P, et al. A comparison of self-organizing neural networks for fast clustering of radar pulses. *Signal Processing*, 1998, 64(3): 249–269.
- [15] ATAA A W, ABDULLAH S N. De-interleaving of radar signals and prf identification algorithms. *IET Radar, Sonar and Navigation*, 2007, 1(5): 340–347.
- [16] GENCOL K, KARA A, AT N. Improvements on de-interleaving of radar pulses in dynamically varying signal environments. *Digital Signal Processing*, 2017, 69: 86–93.
- [17] TSCHEREPANOW M, KORTKAMP M, KAMMER M. A hierarchical ART network for the stable incremental learning of topological structures and associations from noisy data. *Neural Networks*, 2011, 24(8): 906–916.
- [18] MATIAS A L S, NETO A R R. On ARTMAP: a fuzzy ARTMAP-based architecture. *Neural Networks*, 2018, 98: 236–250.
- [19] KESKIN G A, ILHAN S, COŞKUN Ö. The fuzzy ART algorithm: a categorization method for supplier evaluation and selection. *Expert System*, 2010, 37(2): 1235–1240.
- [20] UNGLERT K, RADIC V, JELLINEK A M. Principal component analysis vs. self-organizing maps combined with hierarchical clustering for pattern recognition in volcano seismic spectra. *Journal of Volcanology and Geothermal Research*, 2016, 320(15): 58–74.
- [21] CHANG C Y, WANG H J, PAN S W. A robust DWT-based copyright verification scheme with fuzzy ART. *Journal of Systems and Software*, 2009, 82(11): 1906–1915.
- [22] ISAWA H, MATSUSHITA H, NISHIO Y. Fuzzy adaptive resonance theory combining overlapped category in consideration of connections. *Proc. of the International Joint Conference on Neural Networks*, 2008: 3595–3600.
- [23] ISAWA H, TOMITA M, MATSUSHITA H, et al. Fuzzy adaptive resonance theory with group learning and its applications. *Proc. of the International Symposium on Nonlinear Theory and its Applications*, 2007: 292–295.
- [24] KIM K B, KIM S. A passport recognition and face verification using enhanced fuzzy ART based RBF network and PCA algorithm. *Neurocomputing*, 2008, 71(16–18): 3202–3210.
- [25] MARA L M L, MINUSSI C R, LOTUFO A D P. Electric load forecasting using a fuzzy ART & ARTMAP neural network. *Applied Soft Computing*, 2005, 5(2): 235–244.
- [26] POURPANAH F, LIM C P, SALEH J M. A hybrid model of fuzzy ARTMAP and genetic algorithm for data classification and rule extraction. *Expert Systems with Applications*, 2016, 49(C): 74–85.
- [27] FURAO S, HASEGAWA O. An incremental network for on-line unsupervised classification and topology learning. *Neural Networks*, 2006, 19(1): 90–106.
- [28] MENDEL J M, JOHN R I B. Type-2 fuzzy sets made simple. *IEEE Trans. on Fuzzy Systems*, 2002, 10(2): 117–127.
- [29] CHOI B I, RHEE C H. Interval type-2 fuzzy membership function generation methods for pattern recognition. *Information Sciences*, 2009, 179(13): 2102–2122.
- [30] KARNIK N N, MENDEL J M. Centroid of a type-2 fuzzy set. *Information Sciences*, 2001, 132(1–4): 195–220.
- [31] MAJEED S, GUPTA A, RAJ D, et al. Uncertain fuzzy self-organization based clustering: an interval type-2 approach to adaptive resonance theory. *Information Sciences*, 2018, 424: 69–90.
- [32] LEONARDO E B D S, ISLAM E, DONALD C W. Dual vigilance fuzzy adaptive resonance theory. *Neural Networks*, 2019, 109: 1–5.

Biographies



JIANG Wen was born in 1991. He received his M.S. degree from Zhengzhou University, China, in 2016. He is currently a doctoral student in School of Information and Electronics, Beijing Institute of Technology (BIT). His research interests include radar signal processing and radar pulses de-interleaving.
E-mail: jwen912@126.com



FU Xiongjun was born in 1978. He received his B.Eng. degree and his Ph.D. degree from Beijing Institute of Technology (BIT), China, in 2000 and 2005 respectively. He is currently the vice dean of the School of Information and Electronics, BIT, and an associate professor and Ph.D. supervisor with BIT. His research interests include radar system, radar signal processing, waveform design, and automatic target recognition.
E-mail: fuxiongjun@bit.edu.cn



CHANG Jiayun was born in 1989. She received her M.S. degree from Beijing Institute of Technology (BIT), China, in 2016. Currently, she is a doctoral student in School of Information and Electronics, BIT. Her research interests include automatic target recognition and radar signal processing.
E-mail: 824400828@qq.com